Biophysical Journal
Article

Biophysical Society

Molecular origins of asymmetric proton conduction in the influenza M2 channel

Themis Lazaridis[1,2,*]
[1]Department of Chemistry, City College of New York/CUNY, New York, New York and [2]Graduate Programs in Chemistry, Biochemistry, and Physics, The Graduate Center, City University of New York, New York, New York

ABSTRACT The M2 proton channel of influenza A is embedded into the viral envelope and allows acidification of the virion when the external pH is lowered. In contrast, no outward proton conductance is observed when the internal pH is lowered, although outward current is observed at positive voltage. Residues Trp41 and Asp44 are known to play a role in preventing pH-driven outward conductance, but the mechanism for this is unclear. We investigate this issue using classical molecular dynamics simulations with periodic proton hops. When all key His37 residues are neutral, inward proton movement is much more facile than outward movement if the His are allowed to shuttle the proton. The preference for inward movement increases further as the charge on the His37 increases. Analysis of the trajectories reveals three factors accounting for this asymmetry. First, in the outward direction, Asp44 traps the hydronium by strong electrostatic interactions. Secondly, Asp44 and Trp41 orient the hydronium with the protons pointing inward, hampering outward Grotthus hopping. As a result, the effective barrier is lower in the inward direction. Trp41 adds to the barrier by weakly H-bonding to potential H^+ acceptors. Finally, for charged His, the H_3O^+ in the inner vestibule tends to get trapped at lipid-lined fenestrations of the cone-shaped channel. Simulations qualitatively reproduce the experimentally observed higher outward conductance of mutants. The ability of positive voltage, unlike proton gradient, to induce an outward current appears to arise from its ability to bias H_3O^+ and the waters around it toward more H-outward orientations.

SIGNIFICANCE The M2 proton channel of influenza A, the best-studied viral ion channel and a proven drug target, conducts protons asymmetrically in response to a pH gradient. That is, protons flow inward when the external pH is low but not outward when the internal pH is low. Experiments identified residues that play a role in this behavior, but how they do it has not been clear. This work identifies three molecular mechanisms that explain qualitatively the experimentally observed preference for inward conduction. These insights could improve our understanding of proton channels and possibly other key biological systems that exhibit vectorial proton transport.

INTRODUCTION

Proton transport through membranes has a central role in bioenergetics (1). All living cells store energy in the form of an electrochemical proton potential, which is subsequently converted to ATP. The proton potential is generated by integral membrane proteins that use light or chemical energy to move protons against their gradient. Although the structures of many proteins involved have been known for quite some time, the mechanisms of these processes are still not fully understood. Proton transport is also key to pH regulation mediated by proton channels (2). Therefore, determining the detailed mechanisms of proton transport would allow the understanding of biochemical systems that are fundamental to life.

The M2 integral membrane protein of influenza A, the best studied member of the viroporin family (3), acts as a proton channel that is activated by low external pH and allows the acidification of the virion in endosomes and the uncoating of the viral genome (4). It also has a role in protecting acid-sensitive hemagglutinin during its transport to the plasma membrane (5). It is a single-pass membrane protein with a helical transmembrane domain that forms tetramers (6). A key residue in the transmembrane domain is His37, which appears responsible for low pH activation and proton selectivity (7,8). Also conserved is a ring of Trp41 residues one helical turn inward from the His37. This channel has attracted considerable experimental and theoretical work, with multiple structures available, from

Submitted October 14, 2022, and accepted for publication November 17, 2022.

*Correspondence: tlazaridis@ccny.cuny.edu

Editor: Marta Filizola.
https://doi.org/10.1016/j.bpj.2022.11.029

solid-state NMR (9,10), solution NMR (11), and crystallography (12–14).

Despite the extensive literature, certain aspects of M2 function are not completely understood. One of the most intriguing observations in M2 electrophysiology is the inability of the channel to conduct protons outward when the inside pH is lowered. Key to this behavior is residues Trp41 and Asp44 as their mutations led to observation of pH-driven outward currents (15,16). The D44N mutation is naturally observed in the Rostock strain and confers increased activity, which compensates for the lower acid stability of that strain's hemagglutinin (17). It has been proposed that the bulky Trp41 residues prevent access of the intraviral protons to the His ring and subsequent outward transport. However, in even the most "closed" M2 structures, the Trp residues seem to leave enough space for H_3O^+ passage. In addition, it is unclear why a conformational change opening the gate would occur only when protons are flowing inward. Other attempts at explaining asymmetric conduction include the directionality of water wires (13) and the relative magnitude of free-energy barriers on the two sides of the His ring (18). In recent work, the loss of asymmetry in the D44N mutant was attributed to the more open structure at the C-terminus and the increased hydration below the His ring, which allows activation from interior protons (19). Finally, the question of why voltage can drive outward current while ΔpH cannot has not yet been addressed.

Here, we study the problem of conduction asymmetry in the M2 channel using a recently proposed algorithm for classical molecular dynamics simulations that allows "Grotthus" hopping of protons from one titratable site to another (20). Using voltage as a biasing force to accelerate H^+ translocation, we perform a large number of short simulations with a proton on either side of the Trp ring and measure the probability of it crossing to the other side. We find asymmetry in proton-crossing probability and identify the physical factors that determine this behavior in wild-type and mutant channels.

MATERIALS AND METHODS

The starting point in this work was the crystal structure of M2 with amantadine (PDB: 6BKK), which belongs to the "C_{closed}" class (14). The inhibitor was deleted, and the M2 tetramer was embedded into a POPC membrane. His37 was either all singly protonated (tautomer τ, or HSE, with proton on Nε, which is four times more populated in solution (21)) or had a total charge of +1 or +2. In the latter case, two diagonally positioned His residues were doubly protonated. We used the CHARMM36 force field for the protein (22) and the lipids (23), a time step of 2 fs, a cutoff of 12 Å for the van der Waals interactions, and particle mesh Ewald (24) for long-range electrostatics. The simulations were run at a constant temperature of 303 K and a constant pressure of 1 bar using the Nose-Hoover and Langevin piston methods. Mutant structures were generated by replacing the Asp44 and/or Trp41 side chain, building the unknown coordinates of the new side chain in a standard geometry, and energy minimizing.

The excess proton was modeled as a classical hydronium (25). The proton-hopping simulations were carried out with the MOBHY module (20) implemented in the program CHARMM (26). Grotthus hopping is enabled by periodic attempts (here, every 10 steps) to move a proton from the current H_3O^+ to a water molecule that is hydrogen bonded to it. Harmonic restraints were used to keep the membrane-protein system at the center of the box, the protein at a certain point in the *xy* plane, and the H3O residues (H_3O^+ and surrounding waters) in a 5-Å cylinder around the channel axis and within ± 27 Å from the membrane center (to prevent them from crossing periodic boundaries). The restraints are needed to prevent vertical shifts of the membrane due to the bias forces (voltage is applied in a region fixed in space) and to maintain the alignment of the H3O with the channel pore.

Because proton conduction through the M2 channel is a slow process (6,27), it needs to be accelerated in some artificial way. For that, we used voltage, which was applied in a 55-Å-wide region across the membrane (28) and felt only by the hydronium and its surrounding water molecules (otherwise the membrane would be destabilized by the high voltage used). The magnitude of the voltage was chosen empirically to be just large enough to start seeing differences in conductance inward and outward or between different mutants. The same bias is applied inward and outward, so it is expected to preserve the relative facility of movement in the two directions. However, it is not possible to recover the correct kinetics and the true absolute conductance from these simulations. Although we use the word "conductance" as equivalent to crossing probability, it should be understood that we are not making rigorous conductance estimates but only compare inward and outward mobility at the same biasing force.

Further details on methods are given in the supporting material.

RESULTS

Inward and outward crossing probabilities in the wild-type channel

After equilibration of the 6BKK crystal structure in a POPC membrane (Fig. 1), a water molecule in the outer vestibule (just below Val27) or below Asp44 was replaced by hydronium, and positive or negative voltage was applied to drive it to the other side. The voltage magnitude was gradually increased until crossing events started to be observed. The protonation state of the His layer was set to either 0 or +2 (Q0, Q2). Five (sometimes 10) 100-ps simulations were performed in each case with different initial velocities. Two options were chosen for the His: allowing or not allowing them to shuttle the proton by protonating and deprotonating.

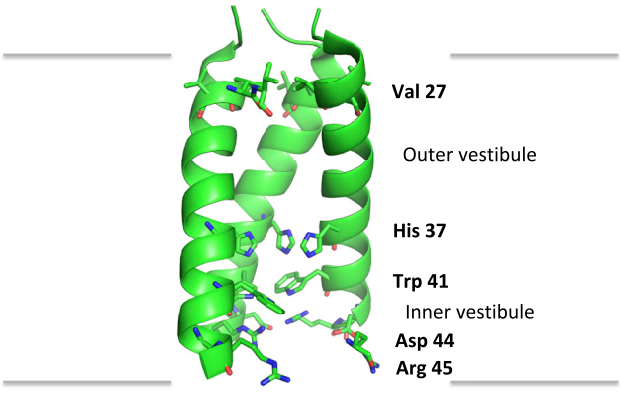

FIGURE 1 The structure of the M2 proton channel (PDB: 6BKK) as embedded in a lipid bilayer. The front helix is omitted for clarity. To see this figure in color, go online.

Table 1 lists the percentage of trajectories that led to successful crossing of H^+ to the other side of the Trp layer.

In the absence of His titration, neither inward nor outward conductance was observed in 100 ps at 5 V. In the inward trajectories, the H^+ remains above the His layer, unable to find a way through other water molecules (the neutral His layer is quite dry). Allowing the His to protonate and deprotonate facilitates significantly the inward movement of the proton. In some cases, the H^+ remains in one of the His or exchanges between the His for the duration of the simulation. In most cases, it detaches and moves to the inner vestibule and beyond. His titration has much less effect on the outward trajectories because the His lie beyond the main barrier, which is the Trp layer. At a higher voltage, conductance is observed in both directions even without His titration.

In the outward trajectories, H_3O^+ is typically bound to the Asp44 side chains, sometimes escaping from one to bind to another (Video S1). Even though Asp44 is salt bridged to Arg45, it still has the ability to engage H_3O^+ with its free CO. Often, the H_3O^+ lies between one Asp and one or two Trp residues and is oriented with the H inward relative to the O (Fig. 2). In the trajectories with successful crossing at higher voltage, the H_3O^+ is able to escape from the Asp and move outward through the Trp side chains. These results suggest a role for Asp44 as a proton trap. Fig. 3 shows time plots of the height and distance from the pore axis of the hydronium in representative inward and outward trajectories.

The Q2-8V trajectories show an even more pronounced asymmetry with or without titratable His. Inward conductance is facile with rapid inward movement of H_3O^+, which stays close to the center of the channel, oriented vertically (dipole parallel to the membrane), approaches one of the deprotonated His and crosses easily the His and the Trp ring by Grotthus hopping through the His (if allowed) or other water molecules (Video S2). In the outward trajectories, H_3O^+ still interacts with the Asp, but the repulsion from the His pushes it to the periphery of the channel, where outward movement is impossible (Video S3). It is remarkable how the same His charge repulsion has such a disparate impact in the two directions (it does, however, slow conduction if the proton starts outside the V-27 gate; see the supporting material).

In the Q2 trajectories, the Trp gate is more open than in the Q0 trajectories. To quantify this, we measured the four indole Nε-Nε (NN) distances between adjacent Trp side chains. In "closed" crystal structures, like the one used here, the Trp side chains are near each other with NN distances of 4.3–5.4 Å. This configuration is maintained in simulations of the neutral His state, but in the Q2 simulations, the NN distances increase (Table 2). The reason for this seems to be the need to hydrate the Nε of the doubly protonated His that points toward the Trp. The water that moves to hydrate the Nε pushes the Trp side chain inward, partially opening the gate (Fig. 4). This provides a mechanism for opening the gate only from the outside. This change in the Trp gate is not accompanied by the opening of the C-terminus, as revealed by the distances between C-terminal carbons in Table 2. The opening of the gate at Q2 is not exploited by the outward trajectories due to trapping of the H^+ at the channel periphery.

TABLE 1 Probability of crossing the Trp layer in the M2 channel as percentage of 5 or 10 100-ps trajectories where crossing is observed

	Without His titration (%)		With His titration (%)	
	Inward	Outward	Inward	Outward
Q0-5 V	0	0	80	20
Q0-8 V	40	30	80	20
Q2-8 V	100	0	100	0

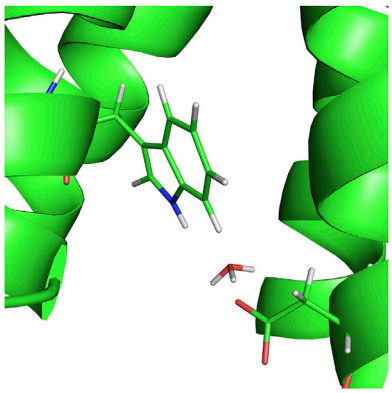

FIGURE 2 Last frame of the outward Q0-5V trajectory depicted in Fig. 3. H_3O^+ trapped between Asp and Trp in M2 during an outward simulation at 5V. To see this figure in color, go online.

Outward crossing probabilities in mutants

Certain mutations of Trp41 and Asp44 are known to allow outward conductance in an outward pH gradient (15,16). We constructed such mutants by replacing the relevant side chains. 100-ns simulations of the mutants as well as the wild type showed modest root-mean-square deviations but significant changes in the Trp gate (see the supporting material). To avoid the uncertainty over the ability of the force field and/or the computational protocol to accurately reproduce the mutants' conformational adaptations, we chose to perform hopping simulations near the crystal structure. In short-timescale simulations, there is no significant change in the opening of the channel or the packing of the Trp gate where it exists (Table 2).

Table 3 shows the outward crossing probability for the wild type and mutants at gradually increasing V. Looking at the Q0 trajectories and Table 3, we can identify three barriers for outward H^+ movement. The highest barrier is escape from Asp44 and starts to be overcome around 8 V. The second barrier is the Trp gate and is overcome around 6.5 V. The third barrier is the lack of hydration below the

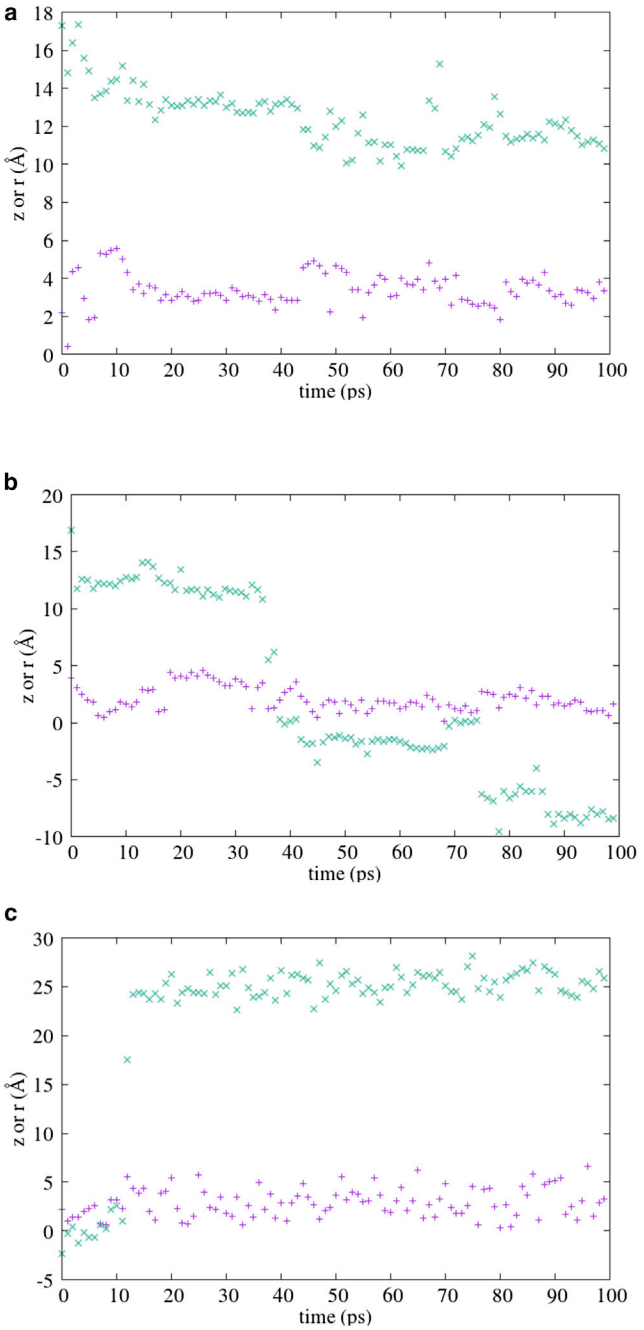

FIGURE 3 Plots of the z coordinate (X symbols) and the distance r from the pore axis (+ symbols) of the hydronium as a function of time for three trajectories: (*a*) Q0-5V outward without His titration (unsuccessful), (*b*) Q0-8V outward without His titration (successful), and (*c*) Q2-8V inward without His titration (successful). To see this figure in color, go online.

His layer and is mostly overcome at about 5 V, although it can also stochastically occur even at higher V. Because the Trp gate barrier is lower than the Asp barrier, we do not observe much difference between wild type and W41F.

In the unsuccessful W41F trajectories, the H_3O^+ stays bound to Asp or escapes from one to bind to another. Its orientation is mostly H-outward, but sometimes it is also vertical or H-inward. One or two hops separate it from water between the Phe side chains, but these hops are apparently too costly energetically. In addition, there is a dry area above the Phe layer.

The barrier function of the Trp gate is most clearly seen in the Q0-5V results for D44N/A where, in the absence of the Asp barrier, the Trp gate reduces the crossing probability from 60% to 0%. Looking at the D44A/N trajectories, we see that there is typically one water molecule between the Trp ("interstitial") and that the H^+ stays one or two hops away from this water. The immediate neighbor of H_3O^+ seems to accept a weak H-bond from a Trp NH, and that disfavors its protonation (Fig. 5). In other snapshots, the H_3O^+ is oriented H-inward and is not even H-bonded to the interstitial water. When Trp is replaced by Phe in the double mutant, there is more space and more water between the Phe side chains so that crossing is less unfavorable.

In the Q2 state, the outward crossing probability of WT and all mutants is 0. Undoubtedly, the repulsion of H^+ by the His plays a role in this. However, the same repulsion also exists in the inward direction but does not prevent crossing. This points to an additional feature of the M2 channel that creates asymmetric conductance. Examination of the outward Q2 trajectories of the double mutant revealed that although there is wide open space between the Phe, the proton tended to reside at the periphery of the inner vestibule (Video S4). The reason for this may be a combination of His repulsion and the known affinity of the excess proton for the water surface and hydrophobic interfaces (29–32). Notably, the outer and inner vestibules in M2 are very different. The outer vestibule is lined by protein (Ser, Gly, Ala). Because of the conical shape, the inner vestibule is more spacious and has fenestrations covered by lipids. H_3O^+ tends to be attracted to these fenestrations, below the Trp or Phe, especially when the His ring is charged. We could call this a hydrophobic trap, in contrast to the electrostatic trap of Asp44. On the channel periphery, as one moves outward, there are fewer water molecules, which makes it more difficult to stabilize the positive charge. This may explain the inward rectification (lower current outward than inward at opposite voltages) observed for the D44A mutant, despite the fact that it allows outward pH-driven proton conductance (33).

Other possible origins for the asymmetry in the W41F/D44A mutant were examined and discounted. The first was the tautomer and conformation of the deprotonated His side chains. The HSE (or τ) tautomer chosen initially points the NH inward. However, replacing HSE with HSD made no difference in the crossing probability. Another possibility was that the repulsion by the Arg45 residues pushed H_3O^+ off center. However, mutation of Arg45 to Ala did not improve conductance but actually reduced it to 0%. The helix dipole could also contribute to directional conductance (34), but this notion is difficult to test (the peptide termini are already neutral in the present simulations).

TABLE 2 Average distances between Trp indole nitrogens and between C-terminal carbon in adjacent helices in the crystal structure (PDB: 6BKK) and over 200-ps molecular dynamics simulations

	NN or <NN>	CC or <CC>
6bkk 4mer 1	4.8	17.7
6bkk 4mer 2	4.6	17.9
WT Q0	5.1 ± 0.5	17.7 ± 0.9
WT Q2	6 ± 0.9	17.8 ± 0.9
W41F Q0	–	17.7 ± 1
D44N Q0	5.1 ± 0.5	18 ± 1.2
D44A Q0	4.9 ± 0.5	17.6 ± 1.2
W41F/D44A Q0	–	17.7 ± 2.2

H_3O^+ orientation around the Trp barrier

Extensive free-energy calculations showed that the largest barrier to H^+ translocation in the M2 channel is at the Trp layer (18,35). In the outward hopping trajectories, we often observed the H_3O^+ to be oriented with the H inward. Because of the directionality of Grotthus hopping, the orientation of H_3O^+ could affect the translocation ability of the excess proton, and voltage could affect its orientation. Therefore, we performed standard simulations without voltage and proton hops, restraining the hydronium to be between the His37 and Trp41 layers ($z = 8$ Å), or between the Asp44 and the Trp41 layers ($z = 12$ Å), and calculated μ_z, the component of the dipole vector parallel to the channel axis. A positive value of μ_z corresponds to H_3O^+ oriented with its H inward relative to the O. From the results in Table 4, we see that when the His is neutral, H_3O^+ between His and Trp is oriented with the H outward, but when the His is charged, its orientation changes to H-inward, as expected. Between Trp and Asp, H_3O^+ is oriented H-inward (Fig. 6). At Q2, the repulsion from the His pushes the H_3O^+ to the periphery of the channel, where it can orient more freely, and that reduces orientational polarization. The primary reason for the H-inward orientation is interaction with the Asp layer and, when present, the His layer charge. The Trp side-chain indole NH groups could also make a contribution. When voltage is applied on the H_3O^+ and the surrounding water molecules and hops are allowed, a variety of orientations are observed, and this is likely related to the ability of H^+ to translocate outward when driven by voltage. Fig. 7 shows the dynamics of μ_z in two cases: Q0 $z = 12$ without voltage and proton hops, and outward simulations at V 5 in the presence of proton hops. When the H_3O^+ is just below the Trp, its orientation is mostly H-inward, with rare fluctuations. Without positional restraint and in the presence of voltage and proton hops, μ_z samples a wide variety of values, and its average is close to 0.

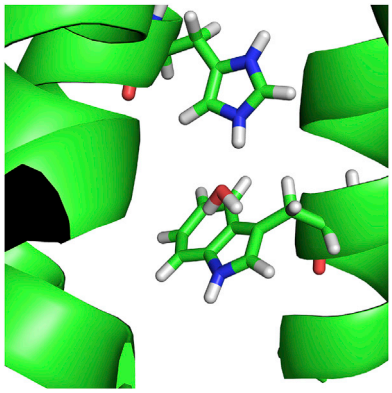

FIGURE 4 Hydration of the Nε of His pushes the Trp side chain inward. To see this figure in color, go online.

DISCUSSION

A number of hypotheses have been proposed to explain the inability of M2 to conduct protons outward upon acidification of the interior. The first was that the Trp side chains provide a steric block during outward conduction but a conformational change opens them during inward conduction (15). The importance of Asp44 was attributed to its ability to maintain the Trp gate in a closed conformation (16). Simulations of the D44N mutant observed a more open and hydrated structure, which was proposed to facilitate outward conductance (19). The relative magnitude of inward and outward barriers was also used to provide a kinetic explanation of asymmetric activation and conductance (18). The present simulations add three new mechanisms: 1) electrostatic trapping by Asp44, 2) orientation of H_3O^+ with the protons inward, favoring inward conduction, and 3) a conical shape that, when combined with repulsion from the His ring, pushes and traps the H_3O^+ to the hydrophobic lining of the inner vestibule. It would be worth exploring whether these mechanisms are exploited in other systems that exhibit vectorial proton transport, such as proton pumps.

Orientation of H_3O^+ is important in this problem. One-dimensional potentials of mean force of an excess proton along the M2 channel provide valuable information (18,19,35) but neglect the directional nature of Grotthus hopping. Standard transition state theory assumes equal probability for a molecule at the top of the barrier to go forward or backward. However, this is not true for Grotthus hopping. Under the situation depicted in Fig. 8, a H_3O^+ would have a much-increased probability of crossing the same hydrophobic barrier from the left than from the right. As a consequence, the effective barrier from the left is significantly lower than that from the right. In addition, because of proton hopping, the H_3O^+ from the left does not even have to reach the top of the barrier, it just needs to be close enough to donate its proton to a water on the other side. It is worth noting that hydronium can change orientation not only by rotation but also by umbrella inversion, which has a barrier of only 1.86 kcal/mol (36). However, a strong field as in Fig. 8 will make inversion highly unfavorable.

TABLE 3 Probability of outward H^+ movement in M2 wild type and mutants at His charge 0 or 2 and different voltages in 100-ps simulations

	Q0-4 V (%)	Q0-5 V (%)	Q0-6.5 V (%)	Q0-8 V (%)	Q2-8 V (%)
WT	–	0	0	30	0
W41F	–	0	20	20	0
D44N	–	0	60	80	0
D44A	–	0	40	80	0
W41F/D44A	0	60	60	80	0

Differences in conformation could contribute significantly to differences in activity between the mutants. Indeed, NMR experiments in detergent micelles indicated changes in the Trp gate in the D44N mutant, and an opening of the structure has been observed in previous simulations (16,19). However, without full experimental structures for the mutants, we would have to rely on the force field and long simulations to produce a structural model. Our 100-ns simulations of the wild type and certain mutants produced reasonably stable structures but also some changes in the Trp gate that affect crossing probabilities (see the supporting material). Experimentally determined mutant structures would be crucial in clarifying the effects of structural adaptations and force field reliability.

It is experimentally established that, in contrast to proton concentration, voltage is able to drive outward conductance in the wild-type M2 channel (15). Based on this, Tang et al. proposed the term gating rather than rectification, although some genuine inward rectification in the current-voltage curves is also observed (33,37). How can voltage drive outward proton current while proton gradient cannot? These two driving forces differ in a number of ways. Voltage is a long-range force that acts on H_3O^+ and every other charge. It could cause subtle conformational adaptations and affect

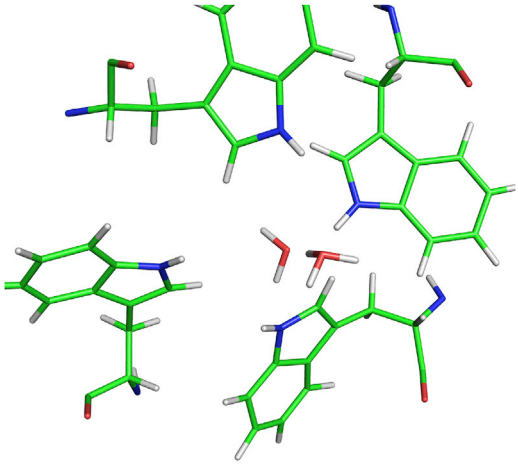

FIGURE 5 Donation of a proton to the interstitial water between the Trp is energetically costly because that water accepts a weak H-bond from Trp. This snapshot is from a D44N trajectory at 5 V where the H_3O^+ is closest to the opening of the Trp gate. To see this figure in color, go online.

TABLE 4 The z component of the hydronium dipole vector at two locations in different His charge states

	z = 8 (His-Trp)	z = 12 (Trp-Asp)
Q0	−1.1 ± 0.6	1.2 ± 0.4
Q1	1.4 ± 0.3	1.2 ± 0.6
Q2	1.4 ± 0.6	0.7 ± 0.5

the protonation and deprotonation rate of His residues. One action of positive voltage that we have observed here is to orient the H_3O^+ and the waters surrounding it with the protons outward, facilitating outward conduction. The energy change upon flipping a single H_3O^+ or H_2O molecule is very small, at values like 60 mV typically used in experiments, but when applied on a large number of molecules over long timescales, it could have a significant effect.

In this work, Asp44 appears to be a stronger barrier than the Trp gate by acting as an electrostatic trap, whereas experimentally, the Trp is known to be at least as important. This could be due to force field inaccuracies, but other explanations are also possible. One is that transient protonation of the Asp44 at low pH could reduce or eliminate its trapping function. In reality, the close approach of a H^+ to a deprotonated Asp could lead to Asp protonation, which is not allowed in the simulations. However, the proximity of Arg45 probably keeps the Asp pK_a low, so we should expect, at best, transient protonation. The present work was done with only one excess proton. If more than one proton is available, one or two could transiently protonate the Asp44, and the others could then proceed more easily to the Trp gate. Preliminary simulations with four excess protons allowing Asp protonation led to protonation of all four Asp44. This will be investigated more extensively in future studies. More experimental work on the Asp44, such as pKa measurements or proton exchange rates by NMR (38), would also be valuable. Finally, the one-dimensional voltage bias we are using may affect somewhat differently the different barriers, i.e., it may be more effective for the Trp barrier than the Asp barrier. It should be noted that Asp44 does not act as a trap in the inward direction: inward trajectories show the H_3O^+ moving all the way past the

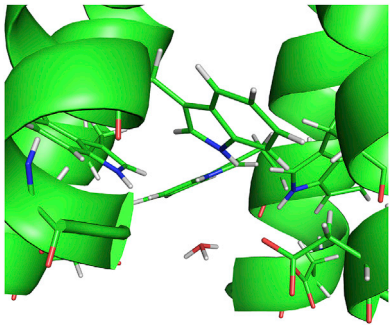

FIGURE 6 In the absence of voltage, H_3O^+ is oriented H-inward between the Asp and Trp layer. This is the last snapshot from a Q0 simulation restraining the H_3O^+ at z = 12 Å. To see this figure in color, go online.

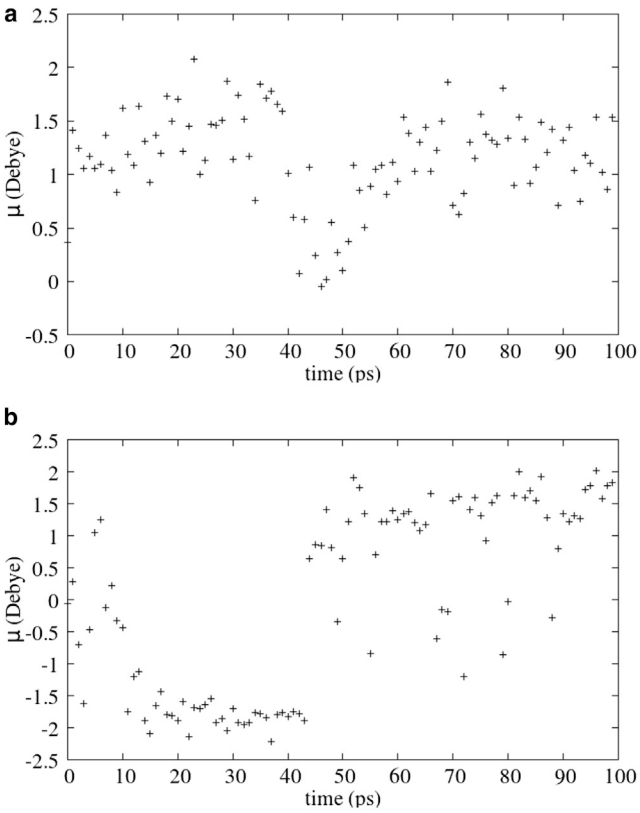

FIGURE 7 Evolution of the z component of the dipole moment in two runs at Q0. (*a*) z = 12 without voltage and proton hops, and (*b*) outward simulations at V 5 in the presence of proton hops (unrestrained z). To see this figure in color, go online.

channel. It is the combination with the Trp barrier that allows the Asp44 to act as a trap in the outward direction.

At equilibrium, without voltage or concentration gradients, the rates of inward and outward movement would be equal (microscopic reversibility). This does not apply to the present nonequilibrium simulations, but if the mechanisms identified could also operate at equilibrium, how could the inward and outward rates be equal? One possibility is that a slower movement outward through the Trp gate could be compensated by a slower movement inward at some other step, such as His deprotonation or proton release to the interior. A detailed account of how all steps and intermediates between interior and exterior are affected by different conditions is needed to completely answer this question.

The main conclusions of this work are qualitative. Calculating actual rates under physiological conditions for a process so slow and so complex is not an easy task. First, one would need to determine the true rate of deprotonation of His. We recently proposed an approach for doing this using classical simulations (39); otherwise, one has to use quantum chemical methods. Second, correction for the effect of bias forces on the rate of H^+ diffusion and the rate of crossing barriers would have to be made. Several approaches are available for these corrections and will be explored in future work. Third, different scenarios for the sequence of events (H^+ movement through water versus His protonation/deprotonation) would have to be evaluated. Finally, proper accounting would have to be made of possible conformational adaptations and their timescales.

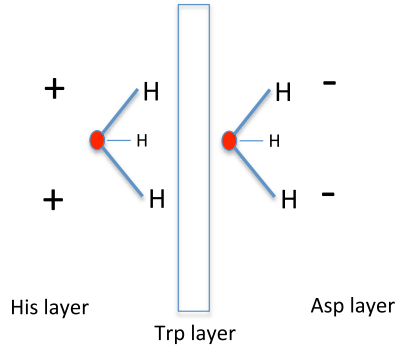

FIGURE 8 Hydronium is oriented by the surrounding charges interacting with its own partial charge distribution (oxygen negative, protons positive). Its orientation affects the probability of the proton to move left or right from the top of a barrier because Grotthus hopping occurs in the direction to which the H^+ points. To see this figure in color, go online.

SUPPORTING MATERIAL

Supporting material can be found online at https://doi.org/10.1016/j.bpj.2022.11.029.

ACKNOWLEDGMENTS

Support by the National Science Foundation (MCB-1855942) is gratefully acknowledged.

DECLARATION OF INTERESTS

The author declares no competing interests.

SUPPORTING CITATIONS

References (40–65) appear in the supporting material.

REFERENCES

1. Nicholls, D., and S. Ferguson. 2002. Bioenergetics 3, 3rd ed. Academic Press, London.
2. DeCoursey, T. E. 2013. Voltage-gated proton channels: molecular biology, physiology, and pathophysiology of the HV family. *Physiol. Rev.* 93:599–652.
3. Nieva, J. L., V. Madan, and L. Carrasco. 2012. Viroporins: structure and biological functions. *Nat. Rev. Microbiol.* 10:563–574.
4. Pinto, L. H., and R. A. Lamb. 2006. The M2 proton channels of influenza A and B viruses. *J. Biol. Chem.* 281:8997–9000.
5. Grambas, S., M. S. Bennett, and A. J. Hay. 1992. Influence of amantadine resistance mutations on the pH regulatory function of the M2 protein of influenza A viruses. *Virology.* 191:541–549.

6. Hong, M., and W. F. DeGrado. 2012. Structural basis for proton conduction and inhibition by the influenza M2 protein. *Protein Sci.* 21:1620–1633.
7. Pinto, L. H., L. J. Holsinger, and R. A. Lamb. 1992. Influenza virus M2 protein has ion channel activity. *Cell.* 69:517–528.
8. Wang, C., R. A. Lamb, and L. H. Pinto. 1995. Activation of the M2 ion channel of influenza virus: a role for the transmembrane domain histidine residue. *Biophys. J.* 69:1363–1371.
9. Sharma, M., M. Yi, H. Dong, H. Qin, E. Peterson, D. D. Busath, H.-X. Zhou, and T. A. Cross. 2010. Insight into the mechanism of the influenza A proton channel from a structure in a lipid bilayer. *Science.* 330:509–512.
10. Cady, S. D., K. Schmidt-Rohr, J. Wang, C. S. Soto, W. F. Degrado, and M. Hong. 2010. Structure of the amantadine binding site of influenza M2 proton channels in lipid bilayers. *Nature.* 463:689–692.
11. Schnell, J. R., and J. J. Chou. 2008. Structure and mechanism of the M2 proton channel of influenza A virus. *Nature.* 451:591–595.
12. Acharya, R., V. Carnevale, G. Fiorin, B. G. Levine, A. L. Polishchuk, V. Balannik, I. Samish, R. A. Lamb, L. H. Pinto, W. F. DeGrado, and M. L. Klein. 2010. Structure and mechanism of proton transport through the transmembrane tetrameric M2 protein bundle of the influenza A virus. *Proc. Natl. Acad. Sci. USA.* 107:15075–15080.
13. Thomaston, J. L., M. Alfonso-Prieto, R. A. Woldeyes, J. S. Fraser, M. L. Klein, G. Fiorin, and W. F. DeGrado. 2015. High-resolution structures of the M2 channel from influenza A virus reveal dynamic pathways for proton stabilization and transduction. *Proc. Natl. Acad. Sci. USA.* 112:14260–14265.
14. Thomaston, J. L., N. F. Polizzi, A. Konstantinidi, J. Wang, A. Kolocouris, and W. F. Degrado. 2018. Inhibitors of the M2 proton channel engage and disrupt transmembrane networks of hydrogen-bonded waters. *J. Am. Chem. Soc.* 140:15219–15226.
15. Tang, Y., F. Zaitseva, R. A. Lamb, and L. H. Pinto. 2002. The gate of the influenza virus M2 proton channel is formed by a single tryptophan residue. *J. Biol. Chem.* 277:39880–39886.
16. Ma, C., G. Fiorin, V. Carnevale, J. Wang, R. A. Lamb, M. L. Klein, Y. Wu, L. H. Pinto, and W. F. Degrado. 2013. Asp44 stabilizes the Trp41 gate of the M2 proton channel of influenza a virus. *Structure.* 21:2033–2041.
17. Betakova, T., F. Ciampor, and A. J. Hay. 2005. Influence of residue 44 on the activity ot the M2 proton channel of influenza A virus. *J. Gen. Virol.* 86:181–184.
18. Liang, R., J. M. J. Swanson, J. J. Madsen, M. Hong, W. F. DeGrado, and G. A. Voth. 2016. Acid activation mechanism of the influenza A M2 proton channel. *Proc. Natl. Acad. Sci. USA.* 112:E6955–E6964.
19. Watkins, L. C., W. F. DeGrado, and G. A. Voth. 2022. Multiscale simulation of an influenza A M2 channel mutant reveals key features of its markedly different proton transport behavior. *J. Am. Chem. Soc.* 144:769–776.
20. Lazaridis, T., and G. Hummer. 2017. Classical molecular dynamics with mobile protons. *J. Chem. Inf. Model.* 57:2833–2845.
21. Reynolds, W. F., I. R. Peat, M. H. Freedman, and J. J. R. Lyerla. 1973. Determination of the tautomeric form of the imidazole ring of L-histidine in basic solution by carbon-13 magnetic resonance spectroscopy. *J. Am. Chem. Soc.* 95:328–331.
22. Best, R. B., X. Zhu, J. Shim, P. E. M. Lopes, J. Mittal, M. Feig, and A. D. MacKerell. 2012. Optimization of the additive CHARMM all-atom protein force field targeting improved sampling of the backbone φ, ψ and side-chain χ1 and χ2 Dihedral Angles. *J. Chem. Theor. Comput.* 8:3257–3273.
23. Klauda, J. B., R. M. Venable, J. A. Freites, J. W. O'Connor, D. J. Tobias, C. Mondragon-Ramirez, I. Vorobyov, A. D. MacKerell, Jr., and R. W. Pastor. 2010. Update of the CHARMM all-atom additive force field for lipids: validation on six lipid types. *J. Phys. Chem. B.* 114:7830–7843.
24. Essmann, U., L. Perera, M. L. Berkowitz, T. Darden, H. Lee, and L. G. Pedersen. 1995. A smooth particle mesh Ewald method. *J. Chem. Phys.* 103:8577–8593.
25. Sagnella, D. E., and G. A. Voth. 1996. Structure and dynamics of hydronium in the ion channel gramicidin A. *Biophys. J.* 70:2043–2051.
26. Brooks, B. R., C. L. Brooks, 3rd, A. D. Mackerell, Jr., L. Nilsson, R. J. Petrella, B. Roux, Y. Won, G. Archontis, C. Bartels, S. Boresch, A. Caflisch, L. Caves, Q. Cui, A. R. Dinner, M. Feig, S. Fischer, J. Gao, M. Hodoscek, W. Im, K. Kuczera, T. Lazaridis, J. Ma, V. Ovchinnikov, E. Paci, R. W. Pastor, C. B. Post, J. Z. Pu, M. Schaefer, B. Tidor, R. M. Venable, H. L. Woodcock, X. Wu, W. Yang, D. M. York, and M. Karplus. 2009. CHARMM: the biomolecular simulation program. *J. Comput. Chem.* 30:1545–1614.
27. Mould, J. A., H. C. Li, C. S. Dudlak, J. D. Lear, A. Pekosz, R. A. Lamb, and L. H. Pinto. 2000. Mechanism for proton conduction of the M2 ion channel of influenza A virus. *J. Biol. Chem.* 275:8592–8599.
28. Mottamal, M., and T. Lazaridis. 2006. Voltage-dependent energetics of alamethicin monomers in the membrane. *Biophys. Chem.* 122:50–57.
29. Petersen, M. K., S. S. Iyengar, T. J. F. Day, and G. A. Voth. 2004. The hydrated proton at the water liquid/vapor interface. *J. Phys. Chem. B.* 108:14804–14806.
30. Iuchi, S., H. Chen, F. Paesani, and G. A. Voth. 2009. Hydrated excess proton at water-hydrophobic interfaces. *J. Phys. Chem. B.* 113:4017–4030.
31. Lee, H. S., and M. E. Tuckerman. 2009. Ab initio molecular dynamics studies of the liquid-vapor interface of an HC1 solution. *J. Phys. Chem.* 113:2144–2151.
32. Duignan, T. T., D. F. Parsons, and B. W. Ninham. 2015. Hydronium and hydroxide at the air-water interface with a continuum solvent model. *Chem. Phys. Lett.* 635:1–12.
33. DiFrancesco, M. L., U. P. Hansen, G. Thiel, A. Moroni, and I. Schroeder. 2014. Effect of cytosolic pH on inward currents reveals structural characteristics of the proton transport cycle in the influenza A protein M2 in cell-free membrane patches of Xenopus oocytes. *PLoS One.* 9.
34. López, G. E., I. Colón-Díaz, A. Cruz, S. Ghosh, S. B. Nicholls, U. Viswanathan, J. A. Hardy, and S. M. Auerbach. 2012. Modeling nonaqueous proton wires built from helical peptides: biased proton transfer driven by helical dipoles. *J. Phys. Chem.* 116:1283–1288.
35. Liang, R., H. Li, J. M. J. Swanson, and G. A. Voth. 2014. Multiscale simulation reveals a multifaceted mechanism of proton permeation through the influenza A M2 proton channel. *Proc. Natl. Acad. Sci. USA.* 111:9396–9401.
36. Rajamäki, T., A. Miani, and L. Halonen. 2003. Six-dimensional ab initio potential energy surfaces for H3O+ and NH3: approaching the subwave number accuracy for the inversion splittings. *J. Chem. Phys.* 118:10929–10938.
37. Chizhmakov, I. V., D. C. Ogden, F. M. Geraghty, A. Hayhurst, A. Skinner, T. Betakova, and A. J. Hay. 2003. Differences in conductance of M2 proton channels of two influenza viruses at low and high pH. *J. Physiol.* 546:427–438.
38. Hu, F., K. Schmidt-Rohr, and M. Hong. 2012. NMR detection of pH-dependent histidine- water proton exchange reveals the conduction mechanism of a transmembrane proton channel. *J. Am. Chem. Soc.* 134:3703–3713.
39. Lazaridis, T., and A. Sepehri. 2022. Amino acid deprotonation rates from classical force fields. *J. Chem. Phys.* 157, 085101.
40. Wei, C., and A. Pohorille. 2013. Activation and proton transport mechanism in influenza A M2 channel. *Biophys. J.* 105:2036–2045.
41. Dong, H., G. Fiorin, W. F. Degrado, and M. L. Klein. 2014. Proton release from the histidine-tetrad in the M2 channel of the influenza A virus. *J. Phys. Chem. B.* 118:12644–12651.
42. Hill, W. G., N. M. Southern, B. MacIver, E. Potter, G. Apodaca, C. P. Smith, and M. L. Zeidel. 2005. Isolation and characterization of the Xenopus oocyte plasma membrane: a new method for studying activity of water and solute transporters. *Am. J. Physiol. Ren. Physiol.* 289:217–224.
43. Ivanova, P. T., D. S. Myers, S. B. Milne, J. L. McClaren, P. G. Thomas, and H. A. Brown. 2015. Lipid Composition of the viral envelope of three strains of influenza virus - not all viruses are created equal. *ACS Infect. Dis.* 1:435–442.

44. Ma, C., A. L. Polishchuk, Y. Ohigashi, A. L. Stouffer, A. Schön, E. Magavern, X. Jing, J. D. Lear, E. Freire, R. A. Lamb, W. F. DeGrado, and L. H. Pinto. 2009. Identification of the functional core of the influenza A virus A/M2 proton-selective ion channel. *Proc. Natl. Acad. Sci. USA.* 106:12283–12288.

45. Caffrey, M., and V. Cherezov. 2009. Crystallizing membrane proteins using lipidic mesophases. *Nat. Protoc.* 4:706–731.

46. Cristian, L., J. D. Lear, and W. F. DeGrado. 2003. Use of thiol-disulfide equilibria to measure the energetics of assembly of transmembrane helices in phospholipid bilayers. *Proc. Natl. Acad. Sci. USA.* 100:14772–14777.

47. Schroeder, C., H. Heider, E. Möncke-Buchner, and T. I. Lin. 2005. The influenza virus ion channel and maturation cofactor M2 is a cholesterol-binding protein. *Eur. Biophys. J.* 34:52–66.

48. Liao, S. Y., K. J. Fritzsching, and M. Hong. 2013. Conformational analysis of the full-length M2 protein of the influenza A virus using solid-state NMR. *Protein Sci.* 22:1623–1638.

49. Kim, S. S., M. A. Upshur, K. Saotome, I. D. Sahu, R. M. McCarrick, J. B. Feix, G. A. Lorigan, and K. P. Howard. 2015. Cholesterol-Dependent conformational exchange of the C-terminal domain of the influenza A M2 protein. *Biochemistry.* 54:7157–7167.

50. Ekanayake, E. V., R. Fu, and T. A. Cross. 2016. Structural influences: cholesterol, drug, and proton binding to full-length influenza A M2 protein. *Biophys. J.* 110:1391–1399.

51. Elkins, M. R., J. K. Williams, M. D. Gelenter, P. Dai, B. Kwon, I. V. Sergeyev, B. L. Pentelute, and M. Hong. 2017. Cholesterol-binding site of the influenza M2 protein in lipid bilayers from solid-state NMR. *Proc. Natl. Acad. Sci. USA.* 114:12946–12951.

52. Martyna, A., B. Bahsoun, J. J. Madsen, F. S. J. S. Jackson, M. D. Badham, G. A. Voth, and J. S. Rossman. 2020. Cholesterol alters the orientation and activity of the influenza virus M2 amphipathic helix in the membrane. *J. Phys. Chem. B.* 124:6738–6747.

53. Zhang, Y., H. X. Zhang, and Q. C. Zheng. 2020. In silico study of membrane lipid Composition regulating conformation and hydration of influenza virus B M2 channel. *J. Chem. Inf. Model.* 60:3603–3615.

54. Wu, E. L., X. Cheng, S. Jo, H. Rui, K. C. Song, E. M. Dávila-Contreras, Y. Qi, J. Lee, V. Monje-Galvan, R. M. Venable, J. B. Klauda, and W. Im. 2014. CHARMM-GUI membrane builder toward realistic biological membrane simulations. *J. Comput. Chem.* 35:1997–2004.

55. Lin, T.-I., and C. Schroeder. 2001. Definitive assignment of proton selectivity and attoampere Unitary current to the M2 ion channel protein of influenza A virus. *J. Virol.* 75:3647–3656.

56. Tieleman, D. P., H. Leontiadou, A. E. Mark, and S. J. Marrink. 2003. Simulation of pore formation in lipid bilayers by mechanical stress and electric fields. *J. Am. Chem. Soc.* 125:6382–6383.

57. Böckmann, R. A., B. L. De Groot, S. Kakorin, E. Neumann, and H. Grubmüller. 2008. Kinetics, statistics, and energetics of lipid membrane electroporation studied by molecular dynamics simulations. *Biophys. J.* 95:1837–1850.

58. Casciola, M., and M. Tarek. 2016. A molecular insight into the electrotransfer of small molecules through electropores driven by electric fields. *Biochim. Biophys. Acta - Biomembr.* 1858:2278–2289.

59. Tokmakoff, A. 2021. Concepts in Biophysical Chemistry. LibreTexts.

60. Hänggi, P., P. Talkner, and M. Borkovec. 1990. Reaction-rate theory: Fifty years after Kramers. *Rev. Mod. Phys.* 62:251–341.

61. Ralph, E. K., and E. Grunwald. 1969. Kinetics of proton exchange in the ionization and acid dissociation of imidazole in aqueous acid. *J. Am. Chem. Soc.* 91:2422–2425.

62. Hummer, G., L. R. Pratt, and A. E. Garcia. 1996. Free energy of ionic hydration. *J. Phys. Chem.* 100:1206–1215.

63. Bignucolo, O., C. Chipot, …, B. Roux. 2022. Galvani Offset potential and constant-pH simulations of membrane proteins. *J. Phys. Chem. B*.

64. Hub, J. S., B. L. De Groot, H. Grubmüller, and G. Groenhof. 2014. Quantifying artifacts in Ewald simulations of inhomogeneous systems with a net charge. *J. Chem. Theor. Comput.* 10:381–390.

65. Chen, W., Y. Huang, and J. Shen. 2016. Conformational activation of a transmembrane proton channel from constant pH molecular dynamics. *J. Phys. Chem. Lett.* 7:3961–3966.